

Transport theory: Spatial coherence of random laser emission

Regine Frank*

Institut für Theoretische Physik, Eberhard-Karls-Universität, 72076 Tübingen, Germany

(Dated: September 15th, 2012)

Recently random laser reached the stage of technological applicability. They have already been engineered as coherent microscope light sources in combination with light transport based disordered lenses. The big issue for all kinds of applications is the degree of coherence of the emitted radiation. The lasing spot sizes in different regimes may provide different degrees of spatial and temporal coherence and as a consequence they can be perfectly tunable light sources for the case that the modal behavior can be controlled easily. In this letter we investigate the spatial coherence lengths of different random laser samples theoretically. The samples only vary in their filling with spherical ZnO Mie scatterers. Beyond we show, that the scattering mean free paths of random lasers are not only a material characteristics and dependent to the filling, instead the mean free paths change in depth of the sample and therefor depend on the nonlinear self-consistent gain of the random lasing principle.

PACS numbers:

INTRODUCTION

Random lasers have been investigated now for almost 15 years, and one would think that they are more or less 'over' now. But everytime they are said to be dead a whole bunch of new ideas and experiments emerge just like the lasing modes emerge on another position in the random laser sample. Both aspects for sure guarantee the fascination of random lasers as playground for theorists as well as experimentalists, however beyond that investigating the actual degree of coherence of random lasing emission is gaining weight now [1, 2]. Besides coherence we discuss the scattering mean free path l_s of random lasers. In literature that scale has often been estimated to be a material characteristics which was independent of the position in the sample. We show that this is actually not the case. The scattering mean free path itself is intrinsically tied to self-consistent nonlinear gain and therefore the spatially dependent dissipative character [5, 6] of the random laser, especially at the surface.

MODEL

The system we consider consists of a randomly scattering medium in the form of the simplest slab geometry [7]. This slab is finite d sized in the z -dimension and assumed of to be of infinite extension in the (x, y) plane. In experimentally relevant situations this refers to film structures of thickness up to $300 \mu\text{m}$ and an in-plane extension of many wavelengths of the used light, i.e. infinitely large. The spherical Mie scatterers [3, 4] are embedded in a homogeneous host material which is in presence considered to be passive. Both, scatterer and host medium, are described by means of a complex dielectric function ϵ_s and ϵ_b , respectively. The scatterers are modeled to be optically active ZnO, with the refractive index to be $n = 9.1$. This sample is optically pumped in order to achieve a sufficient electronic population inversion within the active medium of the scatterers by means of an inci-

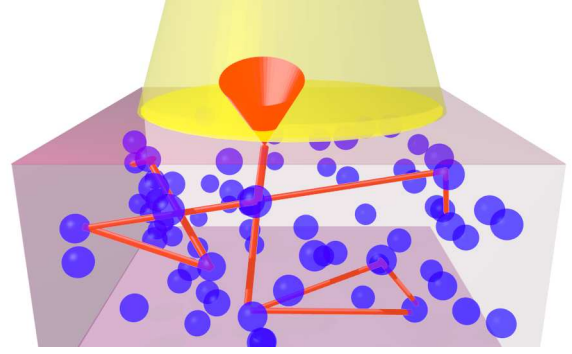


FIG. 1: ZnO spherical Mie scatterers at random locations (blue) are optically pumped from above (wide yellow beam). The pumping yields an inversion of the atomic occupation number within the ZnO causing stimulated emission of light (orange light paths). The emitted intensity multiply scatters and concentrates due to the samples density distributions. At the laser threshold the system experiences a phase transition and second order coherent intensity escapes the system through its surfaces (orange cone). The scatterers radius is $r_0 = 600\text{nm}$, $\lambda = 723\text{nm}$ and the samples finite dimension is of $d = 32\mu\text{m}$.

dent pump laser, perpendicular onto the (x, y) -surface of the random laser. The laser feedback is guaranteed by multiple scattering. The same mechanism actually supports stimulated emission and hence coherent light intensity within the setup. The so generated laser intensity then may leave the sample through both open surfaces of the sample geometry, the dissipation channels. The emitted light is eventually observed at the surface of the sample in the form of lasing spots which comprise to a lasing mode. These lasing modes are of a characteristic size depending on system parameters such as scatterer size, wavelength of the pump source, filling fraction and film thickness etc..

This mode size, i.e. the intensity correlation or coherence length of the coherently emitted laser intensity, is derived by means of field theoretical approach based on the electronic

localization theory by Vollhard and Wölfe [8].

THEORY

The equation of motion for the electric field of stimulated emitted light $\Psi_\omega(\vec{r})$ within the sample is given by the wave equation

$$\frac{\omega^2}{c^2} \epsilon(\vec{r}) \Psi_\omega(\vec{r}) + \nabla^2 \Psi_\omega(\vec{r}) = -i\omega \frac{4\pi}{c^2} j_\omega(\vec{r}), \quad (1)$$

where we denote c to be the vacuum speed of light and $j_\omega(\vec{r})$ the external source. The dielectric constant $\epsilon(\vec{r}) = \epsilon_b + \Delta\epsilon V(\vec{r})$, where the dielectric contrast has been defined according to $\Delta\epsilon = \epsilon_s - \epsilon_b$. It describes the random arrangement of scatterers in terms of $V(\vec{r}) = \sum_{\vec{R}} S_{\vec{R}}(\vec{r} - \vec{R})$, with $S_{\vec{R}}(\vec{r})$ a localized shape function at random locations \vec{R} . The intensity correlation function is then related to the field-field-correlation function Φ , often referred to as the four-point-correlation, $\Phi = \langle \Psi(\vec{r}, t) \Psi^*(\vec{r}', t') \rangle$. Here, the angular brackets $\langle \dots \rangle$ refer to the disorder average or ensemble average of this random system. In order to calculate the field-field-correlation Φ the Green's function formalism is best suited.

The (single-particle) Green's function is related to the (scalar) electrical field, Eq. (1) by

$$\Psi(\vec{r}, t) = \int d^3r' \int dt' G(\vec{r}, \vec{r}'; t, t') j(\vec{r}', t'). \quad (2)$$

In order to study the transport of the above introduced field-field-correlation we consider the 4-point correlation function, defined now in terms of the non-averaged Green's functions, i.e. the retarded \hat{G} and the advanced Green's function \hat{G}^* , where now we find $\Phi \sim \langle \hat{G} \hat{G}^* \rangle$.

The intensity correlation obeys an equation of motion itself, the Bethe-Salpeter equation (BS), given in coordinate space given as

$$\begin{aligned} \Phi(r_1, r'_1; r_2, r'_2) &= G^R(r_1, r'_1) G^A(r_2, r'_2) \\ &+ \sum_{r_3, r_4, r_5, r_6} G^R(r_1, r_5) G^A(r_2, r_6) \times \\ &\times \gamma(r_5, r_3; r_6, r_4) \Phi(r_3, r'_1; r_4, r'_2). \end{aligned} \quad (3)$$

In the BS, we introduced the irreducible vertex function $\gamma(r_5, r_3; r_6, r_4)$ which represents the scattering interactions of the intensity correlation inside the disordered medium of finite size [9]. The irreducible vertex is discussed in the given reference in detail.

To account for the particular form of the system geometry, Wigner coordinates are chosen, in which a full Fourier transform of the spatial coordinates within the infinitely extended (x, y) -plane is used, where we use relative $\vec{q}_{||} = (q_x, q_y)$ and

center-of-mass momentum $\vec{Q}_{||} = (Q_x, Q_y)$ variables. However, the finite z -coordinate of the slab is transformed into relative and center-of-mass real-space coordinates, i.e. z and Z respectively. In this representation only the relative coordinate is Fourier transformed. This procedure is justified because the relative coordinates of the intensity correlation are related to the scale of the oscillating electric field, whereas the center-of-mass coordinates are related to the scale of the collective behavior of the intensity, which is a significantly larger scale. Given that the thickness of the slab is much larger than the wavelength of the laser light as discussed above, a Fourier transform with respect to this perpendicular relative coordinate is perfectly acceptable.

In this representation the BS equation, Eq. (3), may be rewritten according to

$$\begin{aligned} &\left[\Delta\Sigma + 2\text{Re}\epsilon\omega\Omega - \Delta\epsilon\omega^2 - 2\vec{p}_{||} \cdot \vec{Q}_{||} + 2ip_z\partial_Z \right] \times \\ &\times \Phi_{pp'}^{Q_{||}}(Z, Z') = \Delta G_p(Q_{||}; Z, Z') \delta(p - p') + \\ &\sum_{Z_{34}} \Delta G_p(Q_{||}) \int \frac{dp''}{(2\pi)^3} \gamma_{pp''}^{Q_{||}}(Z, Z_{34}) \Phi_{p''p'}^{Q_{||}}(Z_{34}, Z') \end{aligned} \quad (4)$$

where we used the abbreviation $\Delta G \equiv G - G^*$. The rewritten BS equation, Eq. (4), also known as kinetic equation, therefore is seen to be a differential equation in finite center-of-mass coordinate Z along the finite thickness of the slab. This differential equation is to be accompanied by respective boundary conditions accounting for the reflectivity of the sample surfaces. Eq. (4) is solved in terms of an expansion of the correlation Φ into its moments, identified as energy density and energy current density correlation, respectively. A self-consistent expression for the diffusion constant is derived, accompanied by a pole structure within the energy density expression.

The lasing behavior in terms of the atomic occupation numbers is incorporated by means of the following laser rate equations

$$\frac{\partial N_3}{\partial t} = \frac{N_0}{\tau_P} - \frac{N_3}{\tau_{32}} \quad (5)$$

$$\frac{\partial N_2}{\partial t} = \frac{N_3}{\tau_{32}} - \left(\frac{1}{\tau_{21}} + \frac{1}{\tau_{nr}} \right) N_2 - \frac{(N_2 - N_1)}{\tau_{21}} n_{ph} \quad (6)$$

$$\frac{\partial N_1}{\partial t} = \left(\frac{1}{\tau_{21}} + \frac{1}{\tau_{nr}} \right) N_2 + \frac{(N_2 - N_1)}{\tau_{21}} n_{ph} - \frac{N_1}{\tau_{10}} \quad (7)$$

$$\frac{\partial N_0}{\partial t} = \frac{N_1}{\tau_{10}} - \frac{N_0}{\tau_P} \quad (8)$$

$$N_{tot} = N_0 + N_1 + N_2 + N_3, \quad (9)$$

where $N_i = N_i(\vec{r}, t)$, $i = 0, 1, 2, 3$ are the population number densities of the corresponding electron level; N_{tot} is the total number of electrons participating in the lasing process, $\gamma_{ij} \equiv 1/\tau_{ij}$ are the transition rates from level i to j , and γ_{nr} is the non-radiative decay rate of the laser level 2.

$\gamma_P \equiv 1/\tau_P$ is the transition rate due to homogeneous, constant, external pumping. Further $n_{ph} \equiv N_{ph}/N_{tot}$ is the photon number density, normalized to N_{tot} .

We are interested in the stationary limit, i.e. $\partial_t N_i = 0$, hence the above system of equations can be solved for the population inversion $n_2 = N_2/N_{tot}$ to yield

$$n_2 = \frac{\gamma_P}{\gamma_P + \gamma_{nr} + \gamma_{21}(n_{ph} + 1)}, \quad (10)$$

where it was assumed that γ_{32} and γ_{10} are large compared to any other decay rate.

In a last step, the laser rate equations are coupled to the microscopic transport theory by identifying the growth term in a photon diffusion with corresponding growth term in the derived equation for the energy density correlation. The equality is ensured by finding an appropriate imaginary part of the scatterers dielectric function ϵ_s for any particular light frequency ω and any position Z within the slab geometry.

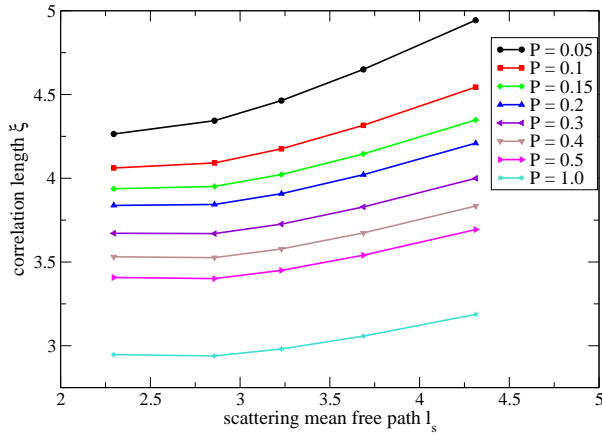


FIG. 2: Calculated coherence length ξ of the random lasing modes as a function of the calculated scattering mean free path l_s . Both length scales are given in units of the scatterer radius r_0 . Different curves correspond to different strengths of the pump intensity P , given in units of transition rate γ_{21} . The different points along a given curve correspond to different filling fractions of the zinc oxide scatterers. The points from left to right correspond to filling fractions of 60%, 50%, 45%, 40%, and 35%.

DISCUSSION

The here developed theory of random lasing includes the regular self-consistency of the Vollhard-Wölfe type for the diffusion coefficient including the interference effects of emitted light intensity. The self-consistent results for the imaginary part of the dielectric coefficient of the laser active scatterers are derived by coupling the mesoscopic transport to semi-classical laser rate equations. The single particle self-energy $\Sigma(\omega)$ entering the single particle Green's function, as in Eq. (1), is approximated as the volume filling fraction of scatterers in the host medium multiplied with the scattering matrix of

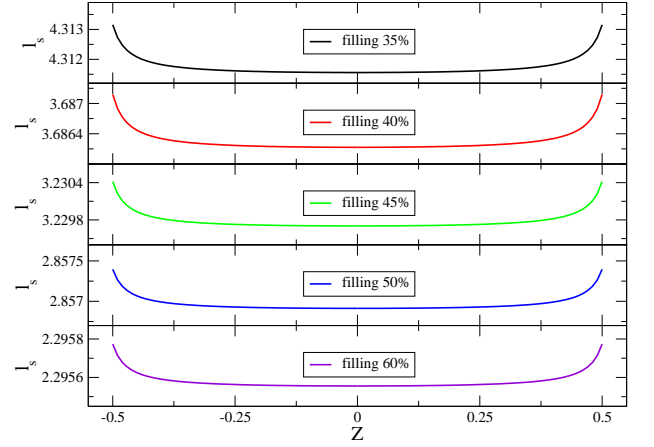


FIG. 3: Calculated scattering mean free path l_s across the depth Z of the random lasing film for various filling fractions as indicated in the legends. The pump rate for all systems is set to be $P = 0.5\gamma_{21}$. The dependence of l_s on the depth originates basically from the depth dependent atomic inversion, i.e. on the depth dependent imaginary part of the dielectric function ϵ_s , which has been self-consistently calculated.

the Mie scatterer. The internal resonances establish threshold friendly parameters.

In Fig. 2 the calculated correlation length ξ , given in units of the scatterer radius r_0 , is presented as a function of the scattering mean free path l_s of the random system. The bullets on the curves correspond to several filling fractions. We find, that the coherence length increases with the mean free paths and again decreases with higher pump intensities. That behavior can be interpreted as self-balancing of sample energy at the threshold. Also in Fig. 2 l_s is given in units of the scatterer radius r_0 . The different curves correspond to different strengths of the pump intensity P , given in units of transition rate γ_{21} .

The displayed points along one graph correspond to numerical evaluations for different filling fractions of the zinc oxide scatterers. In particular, the points from left to right correspond to filling fractions of 60%, 50%, 45%, 40%, and 35%. The correlation or coherence length is found to decrease with increasing pump intensity. Further, the dependence on the scattering mean free path is decreased for stronger pumping. This is in agreement with recent experimental results, as discussed in reference [1].

The discussed coherence length at the surface of the sample, Fig. 2, has also been calculated across the sample thickness. In Fig. 4, the coherence length ξ for a volume filling fraction of the scatterer of 40% and a pump rate of $P = 0.1\gamma_{21}$ is shown in the upper panel. This is accompanied by the calculated photon number density in the middle panel as well as the scattering mean free path l_s as a function of the sample depth Z . The variation of the mean free path is especially noteworthy since it is solely dependent on the different material inversion in center of the film and close to the surfaces. Depth dependent measurements of the scattering mean free path of pumped laser active media have not been reported so

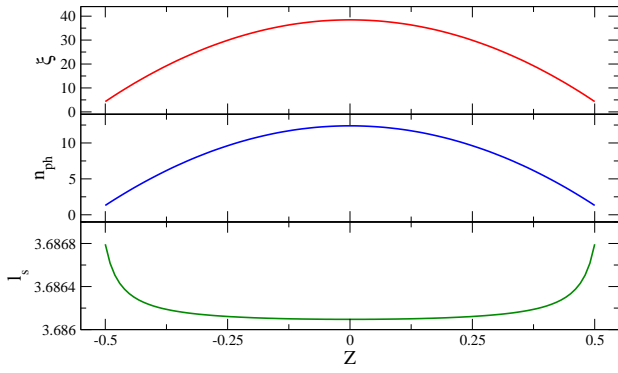


FIG. 4: Calculated coherence length ξ , photon number density n_{ph} and scattering mean free path l_s across the slab geometry from surface to surface. The parameter set is a filling fraction of 40% and a pump rate of $P = 0.1\gamma_{21}$.

far.

CONCLUSION

In summary, we considered a system of randomly positioned laser active ZnO scatterers and we developed a systematic theory for random lasing in finite sized disordered systems. The self-consistent theory of light localization, including interference effects of the emitted laser intensity, is coupled to the laser rate equation in order to obtain the corresponding nonlinear gain of the lasing system. The calculated

averaged correlation or coherence length of the occurring lasing spots is systematically studied and found to exhibit a characteristic dependence on the scattering mean free path of the sample in dependency to the in-depth position. These results are in agreement with recent experimental findings.

ACKNOWLEDGEMENT

The author thanks H. Cao, F. Hasselbach, H. Kalt, B. Redding and C. Lienau and his group for valuable discussions.

* Electronic address: r.frank@uni-tuebingen.de

- [1] B. Redding, M. A. Choma, H. Cao, *Optics Letters* **36**, 3404 (2011).
- [2] S. Aberra Guebrou, C. Symonds, E. Homeyer, J. C. Plenet, Yu. N. Gartstein, V. M. Agranovich, J. Bellessa, *Phys Rev Lett* **108**, 066401 (2012).
- [3] G. Mie, *Annalen der Physik*, **4**, 25, 377-445 (1908).
- [4] K. L. van der Molen *et al.*, *Opt. Lett.* **31**, 1432 (2006).
- [5] J. Fallert, R. J. B. Dietz, J. Sartor, D. Schneider, C. Klingshirn, H. Kalt, *Nature Photonics* **3**, 279 (2009).
- [6] R. Frank, A. Lubatsch, *Proceedings of SPIE* **8095**, 80950R (2011);
- [7] D. S. Wiersma, *Nature Physics* **4**, 359 (2008).
- [8] D. Vollhardt and P. Wölfle, *Phys. Rev. B* **22**, 4666 (1980).
- [9] R. Frank, A. Lubatsch, *Phys. Rev. A* **84**, 013814 (2011).
- [10] Corresponding author E-mail: r.frank@uni-tuebingen.de